Research on Engineering Structures & Materials
www.jresm.org
MIM Research Group

Research Article

Investigating the constraint role in *J-CTOD* relationship for compact tension (CT) specimen

Nagaraj Ekabote[a]

School of Mechanical Engineering, KLE Technological University, Hubli, India

Article Info

Article history:

Received 19 Apr 2024
Accepted 03 July 2024

Keywords:

CTOD;
J-integral;
Constraint factor (m);
ASTM 1820;
45^0 intercept method

Abstract

The Crack Tip Opening Displacement (CTOD or δ) estimation from J-integral (J) defined by ASTM 1820 considers the CTOD dependency on material properties, and the constraint factor (m). The m in Compact Tension (CT) specimen is based on yield to tensile strength ratio (σ_{ys}/σ_{ut}) without taking into account of in-plane dimensions as in Single Edge Notch Bending (SENB). Hence, an attempt is made to understand the effect of crack length to specimen width (a/W), specimen thickness to specimen width (B/W) for different σ_{ys}/σ_{ut} on CTOD using CT specimen. A new method of estimating the CTOD from FE analysis is demonstrated and validated with 45^0-intercept method. It has been found that the ASTM 1820 based CTOD (δ_{ASTM}) assessed values under-estimate the actual CTOD present in the CT specimen. The variation in a/W and B/W doesn't affect the J-CTOD relationship as stated by ASTM 1820. However, the CTOD measured by FE analysis (δ_{FE}) are consistently higher than the δ_{ASTM}. Therefore, an effort is made to correct the constraint factor, m based on present FE analysis by considering the effect of σ_{ys}/σ_{ut}. The proposed corrected constraint factor, m_{FE}, can be employed in fracture applications that generally need both the J-integral and the CTOD.

1. Introduction

Stress intensity factor (K_I) and *J*-integral (*J*) are the common fracture parameters used to determine the crack behavior in elastic and elastic-plastic materials, respectively. The K_I (stress-based parameter) and *J* (energy-based parameter) are determined using the applied load, Crack Mouth Opening Displacement (*CMOD*), and crack length (*a*) increment. Similarly, Crack Tip Opening Displacement (*CTOD*) is the oldest fracture toughness parameter used for fracture assessment of pipelines, pressure vessels, and oil and gas industries [1, 2]. *CTOD* is the displacement-based parameter, and its direct relation with micro mechanisms of dislocations among the grains to characterize the material is an advantage over other fracture toughness parameters [3, 4]. However, unlike K_I and *J* evaluation, the acceptance of *CTOD* is deprived, owing to its distinct estimation methods adopted by different standards. The under and over-estimation of actual *CTOD* by these standards led to restricting the *CTOD* application as a characterizing fracture parameter.

CTOD, refers to the displacement of the original crack tip in the direction of the applied force. The Plastic Hinge Method (PHM) and *J*-based *CTOD* techniques were adopted by different standard bodies for critical *CTOD* measurement (δ_{IC}). *CTOD* measurements derived from PHM-based technique were accepted by the Japan Welding Engineering Society (JWES) and British Standard Institution (BSI) standards. The literature [1, 5-7]

Corresponding author: nagaraj_ekbote@kletech.ac.in, ekabotenagaraj@gmail.com
[a]orcid.org/0000-0002-5711-7416
DOI: http://dx.doi.org/10.17515/resm2024.251me0419rs

revealed the PHM-based measured *CTOD*'s vulnerability towards the specimen's geometry and material property. The researchers [5-7] recommended modifying the PHM-based *CTOD* equation accounting for various specimen geometry and material properties. Experimental *CTOD* values validated these modifications in the equations of the *CTOD*. However, the standard bodies have yet to recommend these modified equations for the critical *CTOD* measurement. Also, the applicability of the modified equations other than Single Edge Notch Bending (SENB) must be verified. Previous studies [6-10] have documented the precise experimental determination of *CTOD* via the digital image correlation (DIC) technique and the silica replica method. However, the time and effort required to measure *CTOD* using these techniques limit its applicability as a fracture parameter.

ASTM 1820 [11] recommends the *CTOD* estimation using experimentally evaluated J as shown in Equation (1). In Equation (1), the σ_Y represents the effective yield strength and m is the constraint parameter. The dependency of m on specimen type and geometry is also acknowledged in Equation (1) for SENB and Compact Tension (CT) specimens. According to ASTM 1820, the m depends on σ_{ys} (yield stress) and σ_{ut} (ultimate stress) along with geometrical constants A_0, A_1, A_2, and A_3. These geometrical constants A_0, A_1, A_2, and A_3 are crack length (a) dependent in SENB but independent in the CT specimen. As per our best knowledge, there is no justification in literature or standards for the non-inclusiveness of the a/W effect on *CTOD* in CT specimen. However, the in-plane constraint variation due to crack length to specimen width (a/W) in the case of CT for other fracture toughness parameters (K_I and J) was well evidenced in the literature [8, 12, 13]. Similarly, the effect of specimen thickness to width (B/W) on fracture toughness and constraint variation [12-15] was reported. Hence, it is essential to investigate the role of specimen geometry variations on *CTOD* using CT specimen.

$$\delta = \frac{J}{m\,\sigma_Y} \tag{1}$$

Where;

$$m = A_0 - A_1 * \left(\frac{\sigma_{ys}}{\sigma_{ut}}\right) + A_2 * \left(\frac{\sigma_{ys}}{\sigma_{ut}}\right)^2 - A_3 * \left(\frac{\sigma_{ys}}{\sigma_{ut}}\right)^3 \tag{2}$$

For SENB;

$$A_0 = 3.18 - 0.22 * \left(\frac{a}{W}\right) \tag{3}$$

$$A_1 = 4.32 - 2.23 * \left(\frac{a}{W}\right) \tag{4}$$

$$A_2 = 4.44 - 2.29 * \left(\frac{a}{W}\right) \tag{5}$$

$$A_3 = 2.05 - 1.06 * \left(\frac{a}{W}\right) \tag{6}$$

For CT;

$$A0 = 3.62,\ A1 = 4.21,\ A2 = 4.33,\ and\ A3 = 2.00 \tag{7}$$

Equation (1) was derived from extensive Finite Element (FE) analysis using 45^0-intercept method to measure the *CTOD* [11] and is applicable for $\sigma_{ys}/\ \sigma_{ut} \geq 0.5$. Kodancha & Kudari

[16] re-evaluated the *J-CTOD* relationship using FE based 45^0 -intercept method and PHM for CT and SENB. It has been concluded that d_n (=$1/m$) factor strongly depends on the *CTOD* estimation technique. Also, the influence of specimen type, applied load, and material on *CTOD* was reported. Similarly, Kittur et al. [17] also noticed the d_n factor and a/W influence on the magnitude of *CTOD* measured as per ASTM 1290 (now this standard is withdrawn) on CT specimen. Further, M. Graba [18] proposed the d_n equation, accounting for the effect of strain hardening, a/W, and applied load on SENB specimen. Tagawa et al. [19] reported that the *CTOD* from ASTM 1290 was 60% lower in SENB compared to the *CTOD* measured from BS 7448 for low σ_{ys}/σ_{ut} steels. Similarly, Kawabata et al. [20] found out the ASTM 1820 based *CTOD* estimation values were 15% lower compared to experimentally estimated *CTOD* in SENB. The effect of σ_{ys}/σ_{ut} on *CTOD* was considered in a newly proposed *CTOD* estimation method to minimize the difference with experimentally measured *CTOD*. Savioli et al. [21] presented the new equations for estimating *CTOD* and *J* in CT specimen with center-line crack welds. The results revealed the dependency of *CTOD* on a/W, strain hardening of the alloy, and strength mismatch ratio. Khor et al. [5] witnessed the inconsistency in *CTOD* values estimated from different standards over a range of σ_{ys}/σ_{ut} in SENB specimen. Kayamori and Kawabata [22] claimed that the *J*-based *CTOD* estimation is more effective in considering the a/W and σ_{ys}/σ_{ut} compared to PHM while using CT specimen.

In the literature [1, 5-7], the researchers and practicing engineers preferred PHM-based *CTOD* estimation over *J*-based *CTOD*. However, the *CTOD* measurement from *the J*-based method is favored at high-temperature applications due to non-dependency on *CMOD* measurement. Also, most *CTOD* measurement techniques were revised to suit SENB rather than CT specimen. In specific applications (like aircraft wings and spars), the CT specimen is appropriate for fracture toughness evaluation and involves extreme temperature variations [23-25]. It is essential to establish a unique and well-accepted relationship between *CTOD* and other popular fracture parameters for the widespread usage of *CTOD* in most applications [1, 5-7, 26]. Overall, the suitability of the *CTOD* estimation method is vital but complex, and hence, a more inclusive and accurate *CTOD* estimation method is essential. This study aims to reassess the implications of a/W, B/W, and σ_{ys}/σ_{ut} on *J*-based *CTOD*, as specified in ASTM 1820, for CT specimens. Further, these implications on the *J*-based *CTOD* equation will be considered for effective constraint inclusiveness.

2. Specimen and Material Details

The three different strain-hardening steels ranging between $0.45 < \sigma_{ys}/\sigma_{ut} > 1$ have been selected from the work of Khor et al. [5, 7]. The chosen steels have σ_{ys}/σ_{ut} of 0.93, 0.72, and 0.48 and are designated further as ST01, ST02, and ST03, respectively. The chosen steel grades will be used to assess the efficiency of the *J*-based *CTOD* equation developed from ASTM 1820, across a wider spectrum of strain hardening. The essential properties of these steel materials are given in Table 1. Typically, a low strain hardening steel have strain hardening exponent (n) less than 0.1, higher σ_{ys}/σ_{ut}, and lower % elongation. The Poisson's ratio (υ) and Elastic modulus (E) are the linear elastic properties.

Table 1. Drill pipe dimensions and properties [4]

Steel category	σ_{ys} (MPa)	σ_{ut} (MPa)	σ_{ys}/σ_{ut}	E (GPa)	υ
ST01	850	914	0.93	217	0.29
ST02	421	585	0.72	205	
ST03	286	595	0.48	205	

Figure 1 displays the typical CT specimen involved for *J* and *CTOD* investigation. The CT specimen has a width (*W*) of 25.4 mm, and the remaining parameters are determined according to the relationship specified in Fig. 1.

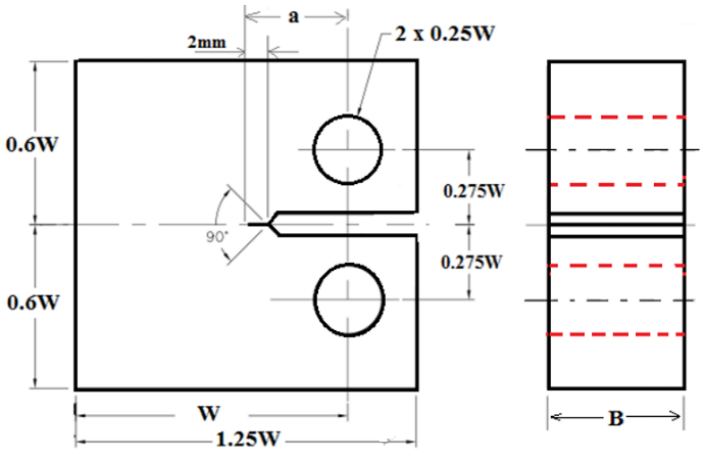

Fig. 1. Standard CT Specimen

To investigate the *a/W*, and *B/W* impact on *J* and *CTOD* fracture parameters, the CT specimens with varied crack length and specimen thicknesses were considered. The *a/W* is varied as 0.45, 0.5, and 0.7, within specified range as per ASTM 1820. Similarly, the thin, standard, and thick specimen effect is considered by varying the *B/W* as 0.25, 0.5, and 1 respectively. The 3-dimensional CT specimens representing the low, medium, and high strain hardening properties, with specimen geometry variations in terms of *a/W* and *B/W* are modelled in ABAQUS software. The 3D models are further processed for elastic-plastic fracture analysis and the details of FE analysis are discussed in further section.

3. Finite Element Analysis

3.1. Meshing and Boundary Conditions

A 3-dimensional non-linear fracture investigation was conducted utilizing ABAQUS 6.14 software. A 3-D half-symmetry CT specimen model was used for analyses. Linear elastic properties (E and υ), and stress-strain post-yield values were input parameters in non-linear fracture analyses. The procedure to input the material properties and stress-strain values into the ABAQUS software was documented in the ABAQUS manual and adopted similarly to the work of Kudari et al. [16]. The symmetrical boundary condition at the un-cracked ligament (*W-a*) and the tensile load along the *y*-direction at the hole was applied, as shown in Fig. 2.

Three-dimensional models with varied *a/W*, *B/W,* and σ_{ys}/σ_{ut} were used in the analyses. 20-noded hexahedral elements with reduced integration (C3D20R) were used for meshing. Near crack area, smaller size elements were utilized to ensure accurate measurement of *CTOD*. The center nodes of the crack adjacent C3D20R elements were advanced in the direction of crack [16, 25]. The movement of these crack adjacent center nodes ensured the natural crack characteristics. Small element size meshes around the crack and relatively coarse mesh far from the crack were utilized for non-linear fracture analysis. The mesh quality was finalized based on converging *J* values and a uniform plasticity distribution around the crack front. Around twenty thousand elements were typically used

for a 3-D symmetric model of $a/W = B/W = 0.5$, of which about 12,000 elements situated at crack surroundings and is shown in Fig. 2.

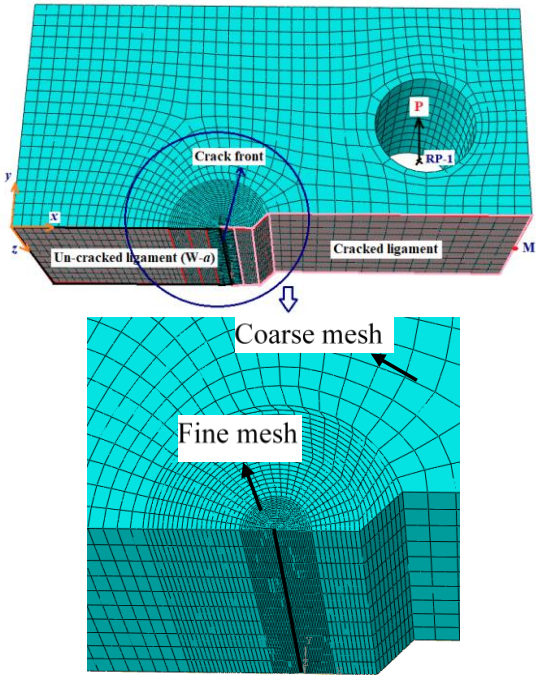

Fig. 2. Three-Dimensional half symmetrical CT model with boundary conditions

3.2. *J*-Integral Extraction and Validation

The direct extraction of *J* values is done from ABAQUS and are similar to the procedure of Kudari et al. [16]. The extracted *J* values are non-linear concerning the load applied. The *CMOD* is the *y*-displacement at the mouth grooves measured through a clip gauge in the fracture toughness experiment. In FE analysis, the *CMOD* can be measured along the loading direction at the mouth groove (point M in Fig. 2). The present non-linear fracture analysis methodology is verified with the Kudari et al. [16] results. The *CMOD* vs. *J* are plotted in Fig. 3 for the CT specimen made of Interstitial Free steel. For a thin specimen, with a/W = 0.5 and W = 20 mm the *J* values are extracted from ABAQUS and used to compare with the Kudari et al. [16] results as plotted in Fig. 3. From Fig. 3, it is confirmed that the results validate the current elastic-plastic fracture procedure, since they significantly coincide with the findings of Kudari et al. [16].

3.3. *CTOD* Extraction and Validation

Similarly, *CTOD* are measured by using 45^0-intercept method (also known as 90^0-intercept method). In this method, along the cracked ligament nodes the displacement in *y*-direction is measured. A typical *y*-displacement of nodes considered along specimen center and surface in the cracked ligament area is shown in Fig. 4. It has been reported that the specimen crack center point possesses the larger *y*-displacement value compare to specimen surface [5, 25]. The measured displacements along the cracked ligament from specimen crack center point are plotted and is shown in Fig. 5. From the origin of the graph, a 45^0 line will be drawn (dotted line in Fig. 5), which will intercept with the *y*-displacement curve (pink line in Fig. 5). The vertical (*y*-direction) distance from the intercept point to

the *x*-axis is termed as *CTOD*/2 as per 45^0-intercept method. Comprehensive FE analysis yields the *J*-based *CTOD*, Equation (1), where the *CTOD* is measured using the 45^0-intercept approach.

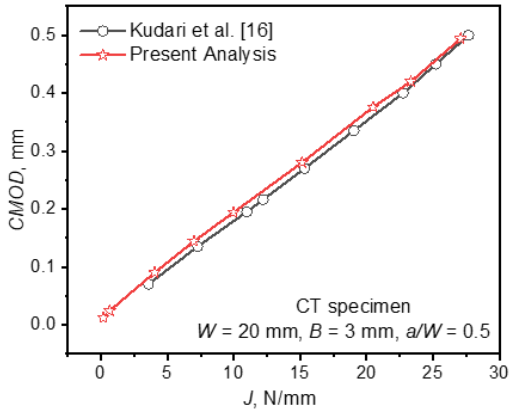

Fig. 3. *J* vs. *CMOD* for thin CT specimen

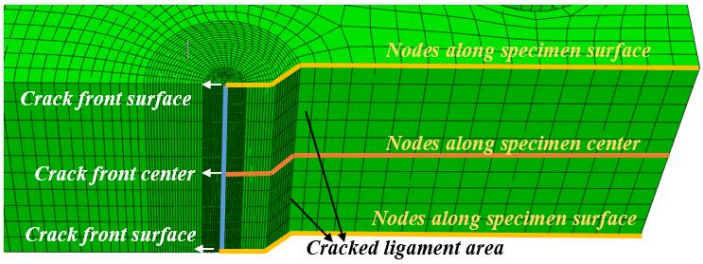

Fig. 4. *J* vs. Cracked ligament area at center and surface

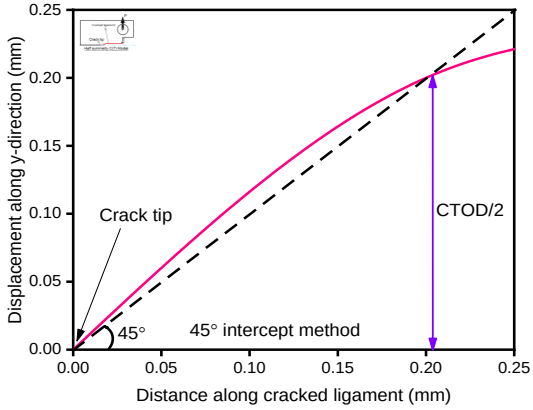

Fig. 5. *CTOD* measurement by 45^0-intercept method

The major limitation of the 45^0-intercept method is its incapability to measure the *CTOD* at lower load magnitudes. Therefore, the *CTOD* at lower loads may be obtained by using Equation (1), which was derived by extrapolating the *CTOD* values. To assess *CTOD* at lower loads, a new *CTOD* estimation approach based on FE analysis is helpful in updating

the value of the constraint parameter in Equation (1). The new technique for measuring the FE-based *CTOD*, its validity and accuracy are discussed in the following section.

3.4. δ_{FE} technique

The $CTOD/2$ value in the δ_{FE} technique is determined by taking the y-displacement of first nearest node from crack front along the cracked ligament direction. Fig. 6 (a) shows the chosen first nearest node along the cracked ligament in the unloaded half-symmetry CT model. For any applied load, the corresponding y-displacement of this chosen node will result in the $CTOD/2$ value as shown in Fig. 6 (b). The proposed δ_{FE} technique seems to be simpler and can be measured directly at chosen single node at cracked ligament.

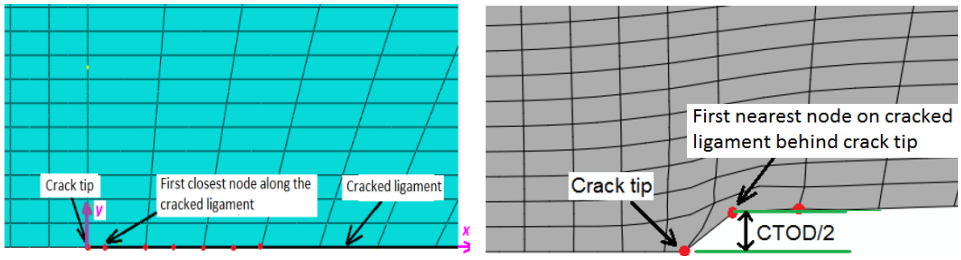

(a) (b)

Fig. 6. *CTOD* measurement by δ_{FE} technique (a) before loading (b) after loading

The accuracy of δ_{FE} technique is measured by comparing with the *CTOD* obtained from 45^0-intercept method (δ_{45}). Fig. 7 shows the *CTOD* measured by the δ_{FE} and δ_{45} techniques with respect to applied stress ratio (applied stress / yield stress = $\sigma_{appl}/\sigma_{ys}$). The nature of *CTOD* variation are non-linear and similar to the J variations. The δ_{FE} technique accurately measured the *CTOD* as similar to the δ_{45} technique for both standard and thick specimens. The δ_{45} technique unable to measure the $CTOD < 0.4$ mm, making it less suitable for lower applied loads. However, δ_{FE} technique accounts the lower *CTOD* values at lower applied loads and *CTOD* measurement is simpler.

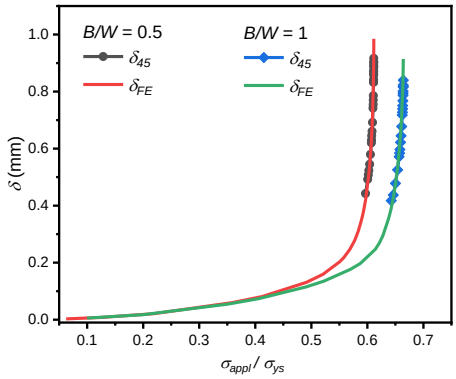

Fig. 7. Comparison of δ_{FE} and δ_{45} techniques

The quality and type of mesh influence on the proposed δ_{FE} technique is verified by introducing the various mesh refinements along the sharp crack front. A fine mesh at crack with up to 0.05 mm gap between crack tip and the first node along the ligament resulted *CTOD* identical (within 2% error) to δ_{45}. As the gap between first node and tip increases more than 0.05 mm, the difference widens for δ_{FE} and δ_{45}. A minimum of 0.05 mm gap may

not result the identical *CTOD* as δ_{45} for some other fracture specimen and mesh quality. Hence, in the absence of comprehensive results on other fracture specimens, one must conduct an extensive FE analysis to define the gap between crack tip and first node. The finer and refined mesh quality near the crack is important in achieving the better *CTOD* value. Also, the smaller elements near the crack ensures the better plasticity distribution. However, the effectiveness of the proposed δ_{FE} technique for blunted cracks used for ductile materials need to be verified. The satisfactory validation depicted in Fig. 7 justifies the adoption of the proposed δ_{FE} technique for subsequent discussions and analysis.

4. Results and Discussions

In this section, the influence of geometry (*a/W*, and *B/W*) and $\sigma_{ys}/\ \sigma_{ut}$ *on J-CTOD* relationship are analyzed. *CTOD* measured from ASTM 1820 will be represented as δ_{ASTM} in further discussions. Both δ_{FE} and δ_{ASTM} are used to analyze the *J-CTOD* relationship.

4.1. δ_{FE} technique

The half-symmetrical CT specimens with *a/W* varying as 0.45, 0.5 and 0.7 are modelled. The standard thickness of *B/W* = 0.5 and the material properties of ST01, ST02, and ST03 are employed in FE analysis. The estimated *CTOD* values as per ASTM 1820 and proposed δ_{FE} technique are shown in Fig. 8. J/σ_Y along the *x*-direction and estimated *CTOD* values along *y*-direction are considered to verify the relation between *J-CTOD*. It has been observed from Fig. 8, that the *a/W* variation has nullifying effect on *CTOD* values measured by both methods for different steel materials considered in the study. However, the δ_{FE} measured values are consistently higher compared to δ_{ASTM} and considered to be improved represented magnitudes of *CTOD* (as validated in Fig. 3). The similar trend of underestimating the actual *CTOD* by δ_{ASTM} compared to PHM are earlier reported [18-20].

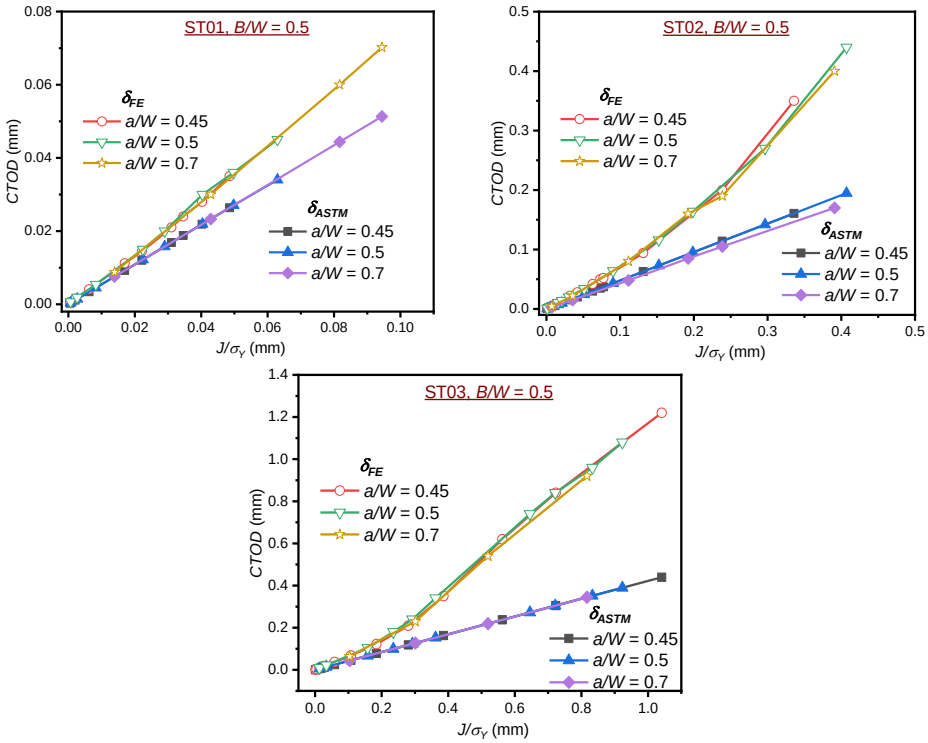

Fig. 8. Effect of *a/W* on *CTOD*

Similarly, the effect of *B/W* on *J-CTOD* relationship is considered and plotted in Fig. 9. Thin, standard, and thick CT specimens are analyzed for standard *a/W* of 0.5. δ_{ASTM} values are unaltered by the varied specimen thickness indicating the effective *J-CTOD* relationship. As similar to Fig. 8, here also the δ_{FE} magnitudes are higher compared to δ_{ASTM} values. The *J* estimation procedure as per ASTM 1820 already imbibes the *a/W* and *B/W* effect and hence a strong relationship is witnessed between *J-CTOD* through unaltered curves for both δ_{ASTM} and δ_{FE}. However, the conservative δ_{ASTM} values shows its incapability to measure the actual constraint near the crack. This major limitation of δ_{ASTM} resulted in almost non-usage of *J*-based *CTOD* in fracture toughness assessments. The enhanced δ_{FE} values over δ_{ASTM} for all *a/W* and *B/W*, signifies a modification required in *J-CTOD* relationship for CT specimen. Hence, the improvised measurement technique to find *CTOD* through FE analysis may enhance the usage of *J*-based *CTOD*.

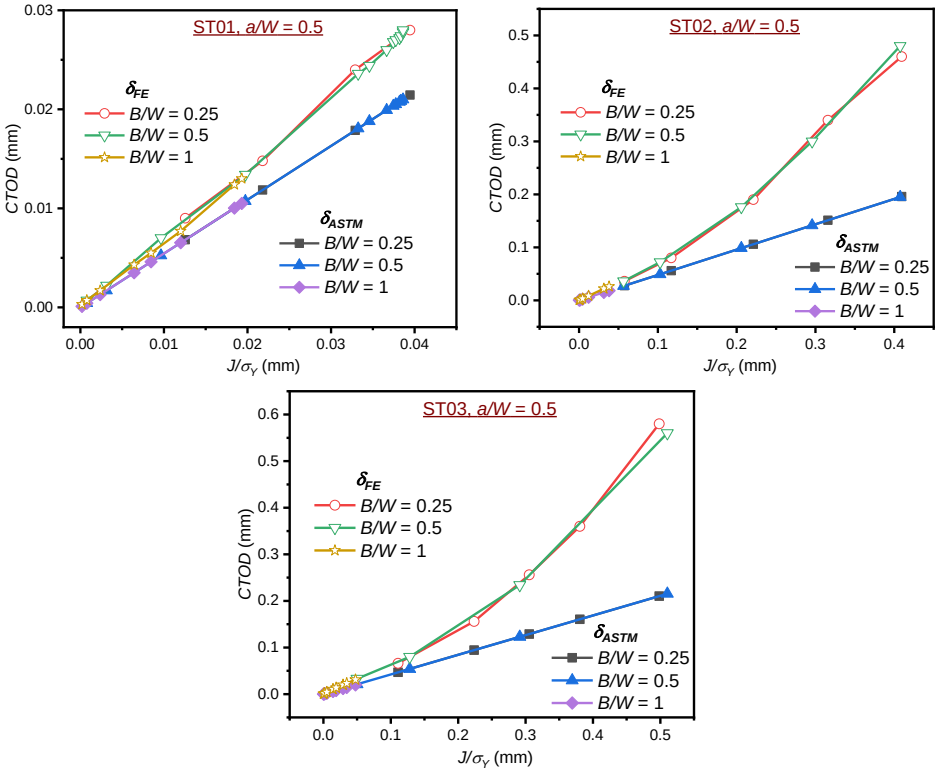

Fig. 9. Effect of *B/W* on *CTOD*

4.2. Effect of σ_{ys}/σ_{ut}

The varied strain hardening of the steel is represented in terms of σ_{ys}/σ_{ut} in the present analysis. Fig. 10 shows the estimated *CTOD* through FE analysis and ASTM 1820 for different strain-hardened steels at *a/W* = *B/W* = 0.5. Here also, the δ_{FE} values are higher over the δ_{ASTM} owing to the conservative constraint factor, *m*. The effect of σ_{ys}/σ_{ut} accounted through constraint factor, *m* equation for CT specimen in ASTM 1820. The higher magnitudes of δ_{FE} specify the better constraint measurement and can be acknowledged through the corrected constraint factor, m_{FE}. A distinction between δ_{ASTM} and δ_{FE} can be made by modifying the constraint factor, *m*, while maintaining the same format of Equation (1). By conducting an in-depth finite element analysis, the influence *a/W*, *B/W*, and σ_{ys}/σ_{ut} is adequately accounted in *J*-based *CTOD* estimation.

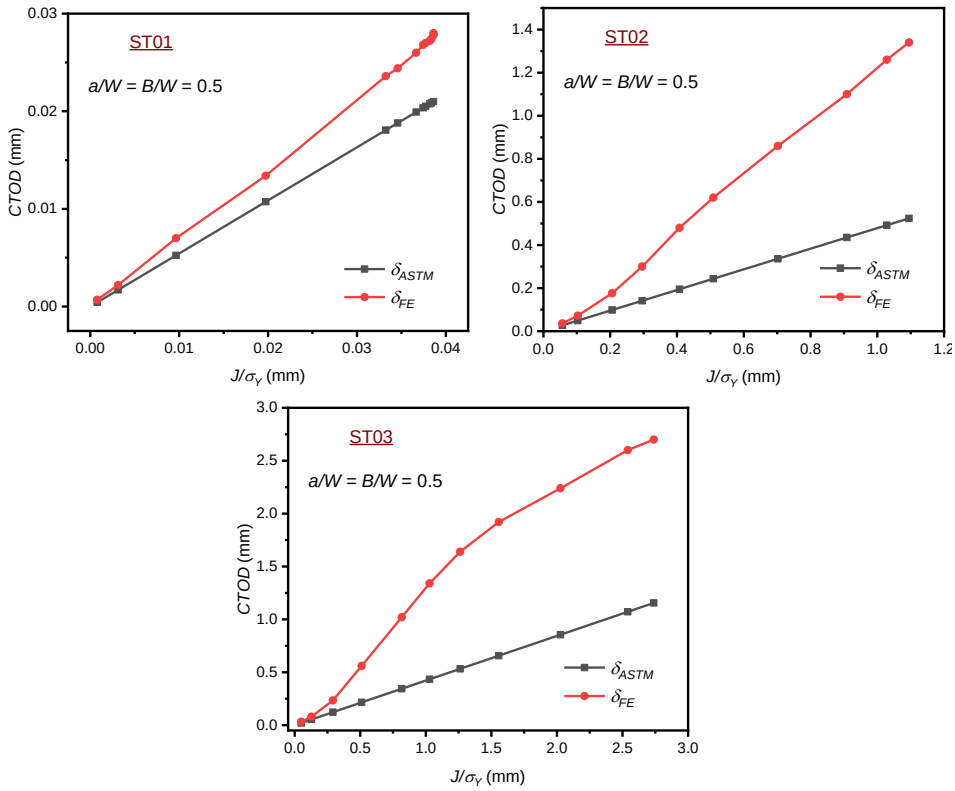

Fig. 10. *CTOD* for different strain hardening materials

The goal is to attain the identical *CTOD* value from PHM and *J*-based *CTOD* methods for a given loading. The reported literature favors the PHM-based standards over *J*-based *CTOD* due to their accuracy with the experimental *CTOD* assessments. However, the unique and recognized relationship among the other fracture toughness parameters is essential for wide acceptance and increased applicability. The interchangeability between fracture toughness parameters, *J* and *CTOD*, provides a strong understanding of non-linear fracture behavior through a constraint perspective. Hence, an attempt is made to extract the slope between J/σ_Y vs. *CTOD* for FE measured values in terms of the constraint factor, *m,* as shown in Fig. 11. The slope is further used to define the corrected constraint factor, m_{FE}, for the actual crack tip/front constraint measurement.

In Fig. 11, the constraint factor, *m,* decreased with increasing σ_{ys}/σ_{ut} and has been defined in ASTM 1820 through the constants A_0, A_1, A_2, and A_3. The cubic polynomial measures the constraint variation due to alteration in σ_{ys}/σ_{ut}. However, the variation of constraint factor, *m,* is linear and has been represented using the straight line as seen in Fig. 11. A cubic equation usage for linear variation of the constraint indicates overestimation and leads to errors. In the present FE analysis, the *m* value increased with an increase in σ_{ys}/σ_{ut}, and also shown the exponential variation with respect to σ_{ys}/σ_{ut}. The extensive FE analysis represented the improved crack constraint measurement resulting in corrected constraint factor, m_{FE} behavior. Thus, an effort is directed to define corrected values of constants A_0, A_1, A_2, and A_3 in the *m* equation. Based on the present FE analysis, the corrected values of constants are A_0 = -2.015, A_1 = -14.750, A_2 = -25.217, *and* A_3 = -14.298.

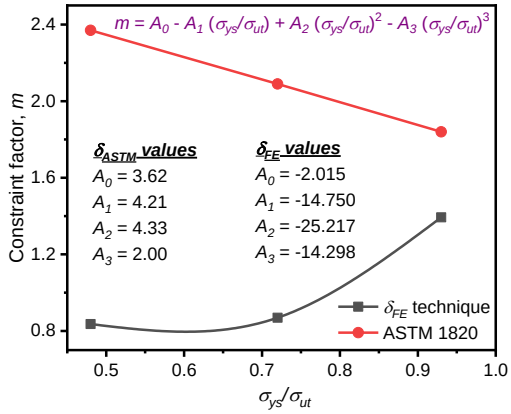

Fig. 11 Constraint factor, m as per ASTM 1820 and FE analysis

Equation (2) may be used to represent the corrected constraint factor, m_{FE}, based on newly suggested constants. The *CTOD* estimated from Equation (2) yielded sufficient accuracy (less than 2% error) compared to δ_{FE}. Equation (8) can be applied to B/W of 0.25 to 1, a/W of 0.45 to 0.7, and $\sigma_{ys}/\sigma_{ut} > 0.45$ to estimate *CTOD* between 0.01 and 1.5 mm. The variations in in-plane (a/W) and out-of-plane (B/W) dimensions align with the ASTM 1820 specified range. Therefore, the applicability of the proposed m_{FE} to different fracture assessments will boost the much-needed correction in ASTM 1820.

$$m_{FE} = -2.015 + 14.750\left(\frac{\sigma_{ys}}{\sigma_{ut}}\right) - 25.217\left(\frac{\sigma_{ys}}{\sigma_{ut}}\right)^2 + 14.298\left(\frac{\sigma_{ys}}{\sigma_{ut}}\right)^3 \quad (8)$$

The PHM based *CTOD* measurement is adopted by European and Japanese fracture toughness related standards. WES 1108 standard utilized the modified PHM to define *CTOD* measurement and is prevalent among the fracture mechanics applications [1, 7]. Unlike δ_{ASTM}, the *CTOD* measured from PHM not related to *J*-integral for its determination. The improvement in determining *CTOD* from corrected constraint factor, m_{FE} is verified for AA2050-T84 alloy having $\sigma_{ys}/\sigma_{ut} = 0.84$. CT specimen is used to understand the fracture behaviour of the aircraft spars and ribs made of AA2050-T84 alloy [23, 25]. Fig. 12 shows the *CTOD* values determined by WES 1108 (shown as $\delta_{\text{WES 1108}}$), ASTM 1820 (shown as $\delta_{\text{ASTM 1820}}$), and proposed δ_{FE} for $a/W = B/W = 0.5$. In the absence of an experimentally measured *CTOD* from DIC or silica replica method, Fig. 12 is useful in justifying the usefulness of δ_{FE}. The *CTOD* determined by ASTM 1820 are the least values due to improper constraint measurement between *J* and *CTOD*. Similarly, the *CTOD* derived by WES 1108 are higher and most *CTOD* based fracture assessment rely on this procedure. The gap between the $\delta_{\text{WES 1108}}$ and $\delta_{\text{ASTM 1820}}$ is larger and therefore the scarce usage of *CTOD* based fracture assessment witnessed in the field. However, the reduced gap between $\delta_{\text{WES 1108}}$ and δ_{FE} will help to relook of both *CTOD* measuring techniques to find efficient way to determine *CTOD* in future. Owing to the proper and efficient FE simulations accounted through corrected constraint factor, m_{FE}, the ASTM may need to re-examine the *J-CTOD* relationship for correction. In the literature, neither the PHM approach nor the *J*-based method can claim to be the correct method for quantifying the true *CTOD* of a CT specimen. However, typical data show that PHM-based *CTOD* measurement tends to overestimate the *CTOD* magnitude [19]. As seen in Fig. 12, the δ_{FE} values appear to be an improved assessment of the constraint at the crack over $\delta_{\text{ASTM 1820}}$. Thus, the suggested corrected constraint factor, m_{FE}, can be used in fracture applications that typically need both the *J*-integral and *CTOD.*

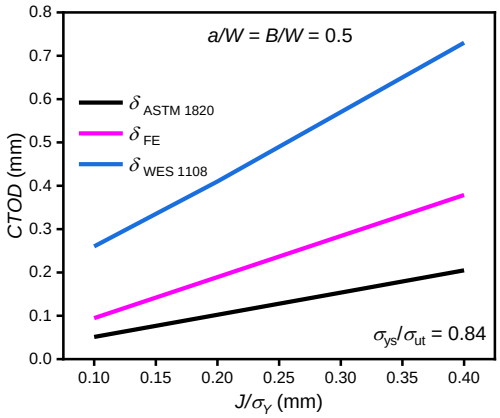

Fig. 12. J/σ_Y vs. *CTOD* by different *CTOD* measuring methods

5. Conclusion

This work primarily addresses the scarce usage of ASTM 1820 recommended *J*-based *CTOD* in fracture toughness assessments of CT specimens. Literature study revealed that the *J*-based *CTOD* equation underestimates the actual *CTOD*. Furthermore, according to ASTM 1820, the constraint at the fracture is determined using a constraint factor, *m*, with the CT specimen's dependence being solely on σ_{ys}/σ_{ut}. The present analysis studies the influence of geometrical variations and σ_{ys}/σ_{ut} on constraint parameter, *m*. The limitation of the 45^0-intercept method and its implications on constraint measurement is addressed by a novel *CTOD* measuring technique, δ_{FE}. The role of geometrical variations is considered by varying *a/W* and *B/W* of the CT specimen within the specified ASTM 1820 recommended range. The varied strain hardening of the material represented in terms of σ_{ys}/σ_{ut} are used to assess the constraint at crack tip/front by in-depth FE analysis. Based on the current research, the following findings may be made.

- A novel *CTOD* measuring technique, δ_{FE} is proposed and validated to measure the lower *CTOD* values. As per our present observations, the proposed δ_{FE} technique seemed simpler and precise for fine mesh quality along the cracked ligament. However, the applicability of the δ_{FE} technique on blunted cracks in the case of ductile material needs to be verified.
- The *J* estimation procedure as per ASTM 1820 already imbibes the *a/W* and *B/W* effect, and hence, a strong relationship is witnessed between *J-CTOD* through unaltered curves for both δ_{ASTM} and δ_{FE}. However, the δ_{FE} magnitudes are consistently higher compared to δ_{ASTM}.
- Improvement in the constraint assessment noticed through δ_{FE} based corrected constraint factor, m_{FE}, with the same *J-CTOD* relation. The proposed corrected constraint factor, m_{FE}, uses the identical cubic polynomial equation as described for constraint factor, *m*, with modified constants as A_0 = -2.015, A_1 = -14.750, A_2 = -25.217, *and* A_3 = -14.298.
- The gap between *J*-based *CTOD* and PHM based *CTOD* can be minimized by using corrected constraint factor, m_{FE}. Hence, the usage of *J*-based *CTOD* can fit the applications demanding both *J*-integral and *CTOD*.
- The corrected constraint factor, m_{FE}, represented through Equation (2), applies to varied crack lengths (*a/W*) between 0.4 to 0.7 for thin, standard, and thick CT specimens with $\sigma_{ys}/\sigma_{ut} > 0.45$ to estimate *CTOD* up to 1.5 mm. Authors believe that

the present work may lead to relooking constraint factor, *m,* for CT specimens by ASTM in future days for better *CTOD*-based fracture toughness assessments.

Acknowledgement

Author thanks the KLE Technological University, Hubballi, for the financial support under the "Capacity Building Project" grants.

References

[1] Khor W. A CTOD equation based on the rigid rotational factor with the consideration of crack tip blunting due to strain hardening for SEN (B). Fatigue & Fracture of Engineering Materials & Structures. 2019 Jul;42(7):1622-30. https://doi.org/10.1111/ffe.13005

[2] Wells AA. Crack opening displacements from elastic-plastic analyses of externally notched tension bars. Engineering Fracture Mechanics. 1969 Apr 1;1(3):399-410. https://doi.org/10.1016/0013-7944(69)90001-0

[3] Ritchie, Robert O., and Dong Liu. Introduction to fracture mechanics. Elsevier, 2021. https://doi.org/10.1016/B978-0-323-89822-5.00008-6

[4] Subramanian, R. Harihara, Subbaiah Arunkumar, Sreekumar Jithin, and Ravi Kiran Bollineni. A critical assessment of J-integral and CTOD as fracture parameters. In Advances in Interdisciplinary Engineering: Select Proceedings of FLAME 2018,429-438. https://doi.org/10.1007/978-981-13-6577-5_41

[5] Khor WL, Moore P, Pisarski H, Brown C. Comparison of methods to determine CTOD for SENB specimens in different strain hardening steels. Fatigue & Fracture of Engineering Materials & Structures. 2018 Mar;41(3):551-64. https://doi.org/10.1111/ffe.12718

[6] Moore, Philippa L., and Wee Liam Khor. The effect of material strain hardening on the determination of CTOD R-curves using SENB specimens. In International Pipeline Conference, vol. 51883, p. V003T05A004. American Society of Mechanical Engineers, 2018. https://doi.org/10.1115/IPC2018-78278

[7] Khor, W., P. L. Moore, H. G. Pisarski, and C. J. Brown. Determination of the rigid rotation plastic hinge point in SENB specimens in different strain hardening steels. In Journal of Physics: Conference Series,IOP Publishin. 2018; 1106(1) 012015. https://doi.org/10.1088/1742-6596/1106/1/012015

[8] Zhu XK, Joyce JA. Review of fracture toughness (G, K, J, CTOD, CTOA) testing and standardization. Engineering fracture mechanics. 2012 May 1;85:1-46. https://doi.org/10.1016/j.engfracmech.2012.02.001

[9] Newman Jr JC, James MA, Zerbst U. A review of the CTOA/CTOD fracture criterion. Engineering Fracture Mechanics. 2003 Feb 1;70(3-4):371-85. https://doi.org/10.1016/S0013-7944(02)00125-X

[10] Vasco-Olmo JM, Diaz Garrido FA, Antunes FV, James MN. Plastic CTOD as fatigue crack growth characterising parameter in 2024-T3 and 7050-T6 aluminium alloys using DIC. Fatigue & Fracture of Engineering Materials & Structures. 2020 Aug;43(8):1719-30.0. https://doi.org/10.1111/ffe.13210

[11] Standard, A.S.T.M., 1820. Standard Test Method for Measurement of Fracture Toughness, West Conshohocken, USA, 2013.

[12] Gupta M, Alderliesten RC, Benedictus R. A review of T-stress and its effects in fracture mechanics. Engineering Fracture Mechanics. 2015 Jan 1;134:218-41. https://doi.org/10.1016/j.engfracmech.2014.10.013

[13] Garcia-Manrique J, Camas D, Gonzalez-Herrera A. Study of the stress intensity factor analysis through thickness: methodological aspects. Fatigue & Fracture of Engineering Materials & Structures. 2017 Aug;40(8):1295-308. https://doi.org/10.1111/ffe.12574

[14] Ekabote, Nagaraj, Krishnaraja G. Kodancha, and S. K. Kudari. Suitability of Standard Fracture Test Specimens for Low Constraint Conditions. In IOP Conference Series: Materials Science and Engineering, vol. 1123, no. 1, p. 012033. IOP Publishing, 2021. https://doi.org/10.1088/1757-899X/1123/1/012033
[15] Meshii T, Tanaka T. Experimental T33-stress formulation of test specimen thickness effect on fracture toughness in the transition temperature region. Engineering Fracture Mechanics. 2010 Mar 1;77(5):867-77. https://doi.org/10.1016/j.engfracmech.2010.01.014
[16] Kudari SK, Kodancha KG. On the relationship between J-integral and CTOD for CT and SENB specimens. Frattura ed Integrità Strutturale. 2008;2(6):3-10. https://doi.org/10.3221/IGF-ESIS.06.01
[17] Kittur, Md Ibrahim, Krishnaraja G. Kodancha, and C. R. Rajashekar. Study of Constraint Issues in Elasto-Plastic Fracture Analysis Using Experimental and Finite Element Simulation. In Turbo Expo: Power for Land, Sea, and Air, vol. 50923, p. V07AT31A009. American Society of Mechanical Engineers, 2017. https://doi.org/10.1115/GT2017-63871
[18] Graba M. Numerical analysis of the influence of in-plane constraints on the crack tip opening displacement for SEN (B) specimens under predominantly plane strain conditions. International Journal of Applied Mechanics and Engineering. 2016 Dec;21(4):849-66. https://doi.org/10.1515/ijame-2016-0050
[19] Tagawa T, Kayamori Y, Ohata M, Handa T, Kawabata T, Yamashita Y, Tsutsumi K, Yoshinari H, Aihara S, Hagihara Y. Comparison of CTOD standards: BS 7448-Part 1 and revised ASTM E1290. Engineering Fracture Mechanics. 2010 Jan 1;77(2):327-36. https://doi.org/10.1016/j.engfracmech.2009.02.009
[20] Kawabata T, Tagawa T, Sakimoto T, Kayamori Y, Ohata M, Yamashita Y, Tamura EI, Yoshinari H, Aihara S, Minami F, Mimura H. Proposal for a new CTOD calculation formula. Engineering Fracture Mechanics. 2016 Jul 1;159:16-34. https://doi.org/10.1016/j.engfracmech.2016.03.019
[21] Savioli RG, Ruggieri C. J and CTOD estimation formulas for C (T) fracture specimens including effects of weld strength overmatch. International journal of fracture. 2013 Jan;179:109-27. https://doi.org/10.1007/s10704-012-9781-4
[22] Kayamori Y, Kawabata T. Evaluation of rotational deformation in compact specimens for CTOD fracture toughness testing. Procedia Structural Integrity. Jan 1;5: 286-93, 2017. https://doi.org/10.1016/j.prostr.2017.07.135
[23] Ekabote, Nagaraj, and Krishnaraja G. Kodancha. Temperature and test specimen thickness (TST) effect on tensile and fracture behavior of AA2050-T84 alloy. Materials Today: Proceedings 59, 673-678, 2022. https://doi.org/10.1016/j.matpr.2021.12.202
[24] Deshpande, Piyush K., Nagaraj Ekabote, and Krishnaraja G. Kodancha. Numerical elastic fracture analysis of SENT test specimen subjected to non-linear loading. Materials Today: Proceedings 2023. https://doi.org/10.1016/j.matpr.2023.09.060
[25] Kodancha K, Ekabote N, Revankar PP. Elastic-plastic fracture analysis of anisotropy effect on AA2050-T84 alloy at different temperatures: A numerical study. Frattura ed Integrità Strutturale. 2022;16(59):78-88. https://doi.org/10.3221/IGF-ESIS.59.06
[26] Antunes FV, Simões R, Branco R, Prates P. Effect of numerical parameters on plastic CTOD. Frattura ed Integrità Strutturale. 2017;11(41):149-56. https://doi.org/10.3221/IGF-ESIS.41.21